Journal of
Materials
Chemistry
www.rsc.org/materials

Organically templated rare earth sulfates with three-dimensional and layered structures†

Meenakshi Dan,[a] **J. N. Behera**[a] **and C. N. R. Rao***[b]

[a]*Chemistry and Physics of Materials Unit, Jawaharlal Nehru Centre for Advanced Scientific Research, Jakkur P. O. Bangalore 560064, India*
[b]*Solid State and Structural Chemistry Unit, Indian Institute of Science, Bangalore 560012, India. E-mail: cnrrao@jncasr.ac.in.; Fax: +91-80-23622766.*

Amine-templated rare earth sulfates of the compositions: $[Ln_2(H_2O)_2(SO_4)_5][C_2N_2H_{10}]_2$, **I**, with Ln = La, Pr or Nd, $[Nd_2(SO_4)_4(H_2O)_2][C_4N_2H_{12}]$, **II**, $[Ln_2(SO_4)_4][C_2N_2H_{10}]$, **III**, with Ln = La or Nd, $[La_2(SO_4)_4][C_3N_2H_{12}]$, **IV** and $[Ln_2(SO_4)_4(H_2O)_4][C_6N_2H_{14}]_2[C_2N_2H_8][SO_4][H_2O]_3$, with **V**, Ln = La, Pr or Nd, have been synthesized under hydrothermal conditions. Both **I** and **II** have three-dimensional architectures with **I** possessing eight-membered apertures surrounding 16-membered apertures, and **II** having 12 membered apertures. Both **III** and **V** have interesting layered structures with LnO_3 layers possessing (6, 3) net topology and the amine located in between the layers. **V** has a layered structure wherein the SO_4 tetrahedra and the LnO_9 polyhedra join together to form (4, 4) net sheets, with two different amines as well as the sulfate ions residing in the interlamellar space.

Introduction

Although metal silicates,[1] phosphates[2] and carboxylates[3] constitute major families of inorganic framework compounds, a start has been made recently to synthesize and characterize open architectures formed by oxyanions such as selenite and sulfate. Thus, layered and three-dimensional selenites have been reported recently.[4] A variety of layered sulfates, especially those of Fe with the kagome structure have been prepared and characterized.[5–7] Sulfates of uranium with different dimensionalities have been reported by O'Hare *et al.*[8] We have been able to prepare several three-dimensional as well as layered, organically templated rare-earth sulfates under hydrothermal conditions. Thus, we have obtained three-dimensional rare-earth sulfates of general formula, $[Ln_2(H_2O)_2(SO_4)_5][C_2N_2H_{10}]_2$, **I**, with Ln = La, Pr or Nd, containing eight-membered apertures surrounded by four 16-membered apertures, possessing the α-Po structure. Another three-dimensional rare earth sulfate of the formula $[Nd_2(SO_4)_4(H_2O)_2][C_4N_2H_{12}]$, **II**, with four 12-membered apertures around each eight-membered aperture, has also been obtained. Both **I** and **II** are uniquely different from the three-dimensional lanthanum sulfate, consisting of only eight-membered apertures, reported recently.[9]

We have prepared several layered rare earth sulfates templated with amines. Thus, a family of rare-earth sulfates, comprising LnO_3 layers with (6, 3) nets,[10] prepared by us, has the composition $[Ln_2(SO_4)_4][C_2N_2H_{10}]$, **III**, with Ln = La or Nd, containing chains of corner-shared four-membered rings which join together by three-coordinated oxygen atoms to form a layer with infinite Ln–O–Ln linkages in two-dimensions. A layered compound of the formula $[La_2(SO_4)_4][C_3N_2H_{12}]$, **IV**, also based on LnO_3 layers, but with the layers formed by the fusion of edge-sharing four-membered ring ladders, has been prepared and characterized. The presence of such infinite Ln–O–Ln linkages in two-dimensions is a noteworthy feature of these layered rare-earth sulfates. Another interesting set of layered compounds of the formula $[Ln_2(SO_4)_4(H_2O)_4]$-$[C_6N_2H_{14}]_2[C_2N_2H_8][SO_4][H_2O]_3$, **V**, Ln = La, Pr or Nd,

containing two different amines and the free sulfate ion has also been synthesized by us. The layer in **V** is formed by the connectivity of the Ln centers by the sulfate units, giving (4, 4) nets with a wave like pattern.[10] The above layer structures are different from those of the lanthanum sulfates reported in the literature,[9,11] analogous Nd derivatives of which have also been prepared by us. In this paper, we describe the synthesis and structures of the three-dimensional and layered rare earth sulfates, **I–V**.

Experimental section

Compounds **I–V** were prepared under hydrothermal conditions. For the synthesis of **I**, **II**, **IV** and **V**, a rare earth chloride solution was prepared by adding the required quantity of concentrated HCl (35% solution) to a suspension of the rare earth oxide in water. In the case of **III**, $LnCl_3$ was used as the staring material. To the solution of the rare-earth chloride, concentrated H_2SO_4 (98% solution) was added dropwise, under constant stirring. The amine was added to the reaction mixture under stirring and the reaction mixture subjected to hydrothermal treatment. Instead of starting from $LnCl_3$, we could start with a solution of Ln_2O_3 in HCl and obtain **III** as the product.

In a typical preparation of **I**, **II**, **IV** and **V**, 250 mg of Ln_2O_3 was dispersed in 4 ml of water, to which 0.4 ml of concentrated HCl (35% solution) was added dropwise with constant stirring. The solution was stirred for 10 more minutes, 0.25 ml of concentrated H_2SO_4 (98% solution) was added dropwise followed by the addition of 0.3 ml of ethylenediamine in the case of **I**, 255.9 mg of piperazine in the case of **II**, 0.192 ml of 1,3-diaminopropane in the case of **IV** and 166.7 mg of 1,4-diazabicyclo[2.2.2]octane (DABCO) in the case of **V**. In preparing **III**, 250 mg of $LnCl_3$ was added to 4 ml of water to form a clear solution, to which 0.1 ml of concentrated H_2SO_4 (98% solution) was added dropwise under constant stirring followed by the addition of 0.045 ml of ethylenediamine. The reaction mixtures of **I–V** were stirred for 30 minutes. The final mixtures were transferred to 23 ml PTFE-lined acid digestion bombs and heated at 150/180 °C for 2–4 days. In the case of **V**, although we started with DABCO, the amine decomposed

† Electronic supplementary information (ESI) available: Tables S1–S6. See http://www.rsc.org/suppdata/jm/b3/b314663d/

under the preparative conditions, partly to give ethylenediamine, which is also accommodated in the structure. The conditions employed for the syntheses of **I** to **V** are listed in Table 1. The products were vacuum filtered and washed with water. The yields generally exceeded 80%. The compounds were characterized by powder X-ray diffraction (XRD) which indicated the products to be new materials and monophasic, the patterns being consistent with the patterns generated from single crystal X-ray diffraction. Energy dispersive X-ray analysis (EDX) gave the expected Ln : S ratios.

The IR spectra of compounds **I** to **V** show the sharp peaks of the amines in the finger print region. The spectra show bands centred around 1050 cm^{-1} and a band in the 600 cm^{-1} region due to the sulfate ion.[11,12] Considering the splittings of these bands, it appears the point group symmetry of the SO_4^{2-} ion is much lower than T_d, probably C_{2v}.

Single crystal structure determination‡

A suitable single crystal of each compound was carefully selected under a polarizing microscope and glued at the tip of a thin glass fiber with cyanoacrylate (super glue) adhesive. Single crystal structure determination by X-ray diffraction was performed on a Siemens Smart-CCD diffractometer equipped with a normal focus, 2.4 kW sealed tube X-ray source (Mo–K_α radiation, $\lambda = 0.71073$ Å) operating at 40 kV and 40 mA. A hemisphere of intensity data was collected at room temperature with ω space scans (width of 0.30° and exposure time of 20 seconds per frame). Pertinent experimental details for the Nd derivatives of **I**, **II**, **III** and **V**, and the La derivative of **IV** are presented in Table 2. The unit cell parameters of the isomorphous rare earth derivatives of **I**, **III** and **V** are listed in Table 3.

Each structure was solved by direct methods using SHELXS-86,[13] which readily established the heavy atom position (Ln, S) and facilitated the identification of the light atoms (O, N, C, H) from difference Fourier maps. An empirical absorption correction based on symmetry equivalent reflections was applied using SADABS programme.[14] All the hydrogen positions were initially located in the difference Fourier maps and the hydrogen atoms were placed geometrically and held in the riding mode for the final refinement. The last cycle of

‡ CCDC reference numbers 224284–224288. See http://www.rsc.org/suppdata/jm/b3/b314663d/ for crystallographic data in .cif or other electronic format.

Table 1 Synthetic conditions for compounds **I** to **V**

	Starting molar composition	°C	Time/days	Formula
I	$Ln_2O_3 + 3$ HCl $+ 3$ $H_2SO_4 + 3$ en^a $+ 4$ ml H_2O	150	2	$[Ln_2(H_2O)_2(SO_4)_5][C_2N_2H_{10}]_2$ (Ln = La, Pr or Nd)
II	$Nd_2O_3 + 3$ HCl $+ 3$ $H_2SO_4 + 4$ PIP^b $+ 4$ ml H_2O	180	4	$[Nd_2(SO_4)_4(H_2O)_2][C_4N_2H_{12}]$
III	$LnCl_3 + 3$ $H_2SO_4 +$ en^a $+ 4$ ml H_2O	150	2	$[Ln_2(SO_4)_4][C_2N_2H_{10}]$ (Ln = La or Nd)
IV	$La_2O_3 + 3$ HCl $+ 3$ $H_2SO_4 + 3$ 1,3-dap^c $+ 4$ ml H_2O	180	2	$[La_2(SO_4)_4][C_3N_2H_{12}]$
V	$Ln_2O_3 + 3$ HCl $+ 3$ $H_2SO_4 +$ DABCO^d $+ 4$ ml H_2O	180	2	$[Ln_2(SO_4)_4(H_2O)_4][C_6N_2H_{14}]_2[SO_4][C_2N_2H_8][H_2O]_3$ (Ln = La, Pr or Nd)

^{a} en = ethylenediamine. ^{b} PIP = piperazine. ^{c} 1,3-dap = 1,3-diaminopropane. ^{d} DABCO = 1,4-diazabicyclo[2.2.2]octane.

Table 2 Crystal data and structure refinement parameters for compounds **I** to **V**

Parameters	**I**	**II**	**III**	**IV**	**V**
Empirical formula	$Nd_2S_5O_{22}C_4N_4H_{24}$	$Nd_2S_4O_{18}C_4N_2H_{16}$	$NdS_2O_8CNH_5$	$La_2S_4O_{16}C_3N_2H_{12}$	$NdS_{2.5}O_{13.5}C_7N_3H_{24}$
Crystal system	Monoclinic	Triclinic	Triclinic	Monoclinic	Orthorhombic
Space group	$P2(1)/c$	P-1	P-1	$P2(1)/c$	$Pbcn$
Crystal size/mm	$0.5 \times 0.15 \times 0.14$	$0.35 \times 0.2 \times 0.18$	$0.5 \times 0.2 \times 0.16$	$0.35 \times 0.4 \times 0.32$	$0.34 \times 0.12 \times 0.15$
a/Å	6.603(1)	6.621(1)	5.482(1)	11.101(1)	25.506(5)
b/Å	16.986(3)	11.794(1)	7.233(1)	7.309(1)	10.102(2)
c/Å	20.412(4)	12.206(1)	9.794(1)	20.132(1)	13.415(3)
α/°	90.0	90.846(1)	87.165(2)	90.0	90.0
β/°	94.845(3)	100.577(1)	83.125(2)	91.829(1)	90.0
γ/°	90.0	102.446(1)	80.269(2)	90.0	90.0
Volume/Å^3	2281.4(7)	913.5(1)	379.86(2)	1632.5(2)	3456.5(11)
Z	4	2	2	4	8
Formula mass	929.05	796.91	367.42	738.21	590.68
ρ_{calc}/g cm^{-3}	2.705	2.897	3.212	3.004	2.270
λ (MoKα)/Å	0.71073	0.71073	0.71073	0.71073	0.71073
μ/mm^{-1}	5.070	6.176	7.402	5.765	3.384
Θ range/°	1.56 to 26.37	1.70 to 23.25	2.10 to 23.18	1.84 to 23.28	1.60 to 28.02
Total data collected	17943	5524	1568	6480	28171
Limiting indices	$-8 \leqslant h \leqslant 8$, $-21 \leqslant k \leqslant 21$, $-22 \leqslant l \leqslant 25$	$-6 \leqslant h \leqslant 7$, $-13 \leqslant k \leqslant 13$, $-13 \leqslant l \leqslant 13$	$-6 \leqslant h \leqslant 5$, $-8 \leqslant k \leqslant 6$, $-10 \leqslant l \leqslant 10$	$-12 \leqslant h \leqslant 12$, $-8 \leqslant k \leqslant 5$, $-22 \leqslant l \leqslant 22$	$-32 \leqslant h \leqslant 32$, $-13 \leqslant k \leqslant 13$, $-17 \leqslant l \leqslant 17$
Unique data	4662	2611	1059	2345	4128
Observed data ($I > 2\sigma(I)$)	4163	2229	970	1922	3745
Refinement method	Full – matrix least squares on $|F^2|$	Full – matrix least squares on $|F^2|$	Full – matrix least squares on $|F^2|$	Full – matrix least squares on $|F^2|$	Full – matrix least squares on $|F^2|$
R_{int}	0.0397	0.0404	0.0209	0.0247	0.0408
R indexes [$I > 2 \sigma(I)$]	$R_1 = 0.0350$, $wR_2 = 0.0696$	$R_1 = 0.0283$, $wR_2 = 0.0660$	$R_1 = 0.0290$, $wR_2 = 0.0750$	$R_1 = 0.0239$, $wR_2 = 0.0643$	$R_1 = 0.0469$, $wR_2 = 0.0913$
R (all data)	$R_1 = 0.0418$, $wR_2 = 0.0720$	$R_1 = 0.0345$, $wR_2 = 0.0679$	$R_1 = 0.0312$, $wR_2 = 0.0765$	$R_1 = 0.0301$, $wR_2 = 0.0666$	$R_1 = 0.0536$, $wR_2 = 0.0932$
Goodness of fit	1.115	0.976	1.071	1.082	1.287
No. of variables	350	287	119	245	274
Largest difference map peak and hole/e Å^{-3}	0.959 and −1.070	1.012 and −1.357	0.733 and −1.333	0.918 and −1.063	0.859 and −1.348

^{a} $R_1 = \sum ||F_o| - |F_c||/\sum |F_o|$. ^{b} $wR_2 = \{\sum [w(F_o^2 - F_c^2)^2]/\sum [w(F_o^2)^2]\}^{1/2}$, $w = 1/[\sigma^2(F_o) + (aP)^2 + bP]$, $P = (F_o^2 + 2F_c^2)/3$, $a = 0.0227$ and $b = 9.6779$ for **I**, $a = 0.0221$ and $b = 0$ for **II**, $a = 0.0515$ and $b = 0$ for **III**, $a = 0.0352$ and $b = 0$ for **IV**, $a = 0.0085$ and $b = 37.0884$ for **V**.

Table 3 Crystal structure data for the other rare-earth metal derivatives of compounds **I**, **III** and **V**

		a	b	c	α	β	γ	Volume/Å^3	Space group
I	Ln = La	6.6180	17.0191	20.4552	90	94.795	90.045	2295.85	P2(1)/c
	Ln = Pr	6.5977	16.9820	20.4067	90	94.929	90	2277.96	P2(1)/c
III	Ln = La	5.4666	7.2065	9.7666	87.037	83.100	80.293	376.34	P-1
V	Ln = La	10.0119	13.2343	25.5112	90	90	90	3470.34	Pbcn
	Ln = Pr	10.1411	13.4893	25.5663	90	90	90	3497.38	Pbcn

Table 4 Selected bond distances in $[Nd_2(H_2O)_2(SO_4)_5][C_2N_2H_{10}]_2$, **I**^{a}

Moiety	Distance/Å	Moiety	Distance/Å
Nd(1)–O(1)	2.424(4)	Nd(1)–O(6)	2.512(4)
Nd(1)–O(2)	2.448(4)	Nd(1)–O(7)	2.568(4)
Nd(1)–O(3)	2.478(5)	Nd(1)–O(8)$^{\#1}$	2.580(4)
Nd(1)–O(4)	2.493(4)	Nd(1)–O(9)	2.615(4)
Nd(1)–O(5)$^{\#1}$	2.503(4)	Nd(2)–O(14)$^{\#3}$	2.502(4)
Nd(2)–O(10)$^{\#2}$	2.442(4)	Nd(2)–O(15)	2.549(4)
Nd(2)–O(11)	2.460(5)	Nd(2)–O(16)	2.549(4)
Nd(2)–O(12)	2.474(4)	Nd(2)–O(17)	2.557(4)
Nd(2)–O(13)	2.479(4)	Nd(2)–O(18)$^{\#3}$	2.693(4)
S(1)–O(19)	1.446(4)	S(1)–O(15)	1.476(4)
S(1)–O(10)	1.464(4)	S(1)–O(12)	1.489(4)
S(2)–O(20)	1.447(4)	S(2)–O(13)$^{\#4}$	1.483(4)
S(2)–O(21)	1.456(4)	S(2)–O(2)	1.487(4)
S(3)–O(16)	1.469(4)	S(3)–O(4)	1.476(4)
S(3)–O(7)	1.470(4)	S(3)–O(17)	1.479(4)
S(4)–O(22)	1.453(4)	S(4)–O(8)	1.472(4)
S(4)–O(1)	1.465(4)	S(4)–O(5)	1.477(4)
S(5)–O(9)	1.461(4)	S(5)–O(14)	1.477(4)
S(5)–O(6)	1.469(4)	S(5)–O(18)	1.478(4)
O(5)–Nd(1)$^{\#2}$	2.503(4)	O(8)–Nd(1)$^{\#2}$	2.580(4)
O(10)–Nd(2)$^{\#1}$	2.442(4)	S(5)–Nd(2)$^{\#3}$	3.2033(14)
O(13)–S(2)$^{\#5}$	1.482(4)	O(18)–Nd(2)$^{\#3}$	2.693(4)
O(14)–Nd(2)$^{\#3}$	2.502(4)	N(3)–C(3)	1.456(8)
N(1)–C(1)	1.481(7)	N(4)–C(4)	1.468(9)
N(2)–C(2)	1.473(8)	C(3)–C(3)$^{\#6}$	1.501(11)
C(1)–C(2)	1.502(8)	C(4)–C(4)$^{\#7}$	1.489(13)

^{a} Symmetry transformations used to generate equivalent atoms: $^{\#1}x + 1, y, z;$ $^{\#2}x − 1, y, z;$ $^{\#3}−x + 1, −y, −z + 1;$ $^{\#4}−x + 1, y + 0.5, −z + 0.75;$ $^{\#5}−x + 1, y − 0.5, −z + 0.75;$ $^{\#6}−x + 2, −y + 1, −z + 1;$ $^{\#7}−x + 2, −y, −z + 1.$

refinement included atomic positions for all the atoms, anisotropic thermal parameters for all the non-hydrogen atoms and isotropic thermal parameters for all the hydrogen atoms. Full-matrix-least-squares structure refinement against $|F^2|$ was carried out using the SHELXTL-PLUS[15] package of

Table 5 Selected bond distances in $[Nd_2(SO_4)_4(H_2O)_2][C_4N_2H_{12}]$, **II**^{a}

Moiety	Distance/Å	Moiety	Distance/Å
Nd(1)–O(1)$^{\#1}$	2.426(4)	Nd(1)–O(6)	2.552(4)
Nd(1)–O(2)$^{\#2}$	2.437(4)	Nd(1)–O(7)	2.555(4)
Nd(1)–O(4)	2.465(5)	Nd(1)–O(2)	2.626(4)
Nd(1)–O(3)	2.466(4)	Nd(1)–O(8)	2.658(5)
Nd(1)–O(5)	2.522(5)	Nd(2)–O(13)$^{\#4}$	2.538(4)
Nd(2)–O(9)$^{\#1}$	2.389(5)	Nd(2)–O(16)$^{\#4}$	2.553(5)
Nd(2)–O(11)$^{\#3}$	2.451(4)	Nd(2)–O(14)	2.558(5)
Nd(2)–O(12)	2.482(4)	Nd(2)–O(15)	2.560(6)
Nd(2)–O(11)	2.536(4)	Nd(2)–O(10)	2.574(4)
S(1)–O(17)	1.440(5)	S(1)–O(14)	1.473(5)
S(1)–O(9)	1.468(5)	S(1)–O(11)	1.524(4)
S(2)–O(6)	1.474(5)	S(2)–O(7)	1.482(5)
S(2)–O(10)	1.480(5)	S(2)–O(12)	1.495(4)
S(3)–O(18)	1.461(4)	S(3)–O(5)	1.478(5)
S(3)–O(1)	1.463(5)	S(3)–O(2)	1.505(5)
S(4)–O(8)	1.468(5)	S(4)–O(3)	1.490(5)
S(4)–O(16)	1.485(5)	S(4)–O(13)	1.490(5)

^{a} Symmetry transformations used to generate equivalent atoms: $^{\#1}−x + 1, −y + 1, −z;$ $^{\#2}−x + 2, −y + 2, −z + 1;$ $^{\#3}−x + 1, −y + 1, −z + 1;$ $^{\#4}x + 1, y, z;$ $^{\#5}x − 1, y, z;$ $^{\#6}−x + 1, −y + 2, −z;$ $^{\#7}−x + 2, −y + 1, −z + 1.$

Table 6 Selected bond distances in $[Nd_2(SO_4)_4][C_2N_2H_{10}]$, **III**^{a}

Moiety	Distance/Å	Moiety	Distance/Å
Nd(1)–O(1)	2.389(4)	Nd(1)–O(6)	2.528(4)
Nd(1)–O(2)	2.427(5)	Nd(1)–O(6)$^{\#2}$	2.543(4)
Nd(1)–O(4)$^{\#1}$	2.490(4)	Nd(1)–O(4)	2.589(5)
Nd(1)–O(3)	2.491(4)	Nd(1)–O(5)$^{\#3}$	2.604(4)
Nd(1)–O(5)	2.525(4)	S(1)–O(5)$^{\#5}$	1.499(5)
S(1)–O(7)	1.442(5)	S(1)–O(6)$^{\#5}$	1.505(4)
S(1)–O(1)	1.483(5)	S(2)–O(3)	1.490(5)
S(2)–O(8)	1.445(5)	S(2)–O(4)	1.496(5)
S(2)–O(2)$^{\#5}$	1.475(5)		

^{a} Symmetry transformations used to generate equivalent atoms: $^{\#1}−x − 1, −y, −z;$ $^{\#2}−x, −y, −z;$ $^{\#3}−x, −y − 1, −z;$ $^{\#4}x + 1, y, z;$ $^{\#5}x − 1, y, z;$ $^{\#6}−x, −y − 1, −z + 1.$

programs. Selected bond lengths in **I–V** are listed in Tables 4–8. The atomic coordinates of **I–V** are provided as supplementary material (Tables S1–S5†). The hydrogen bond parameters in **I–V** are as supplementary information, table S6.†

Table 7 Selected bond distances in $[La_2(SO_4)_4][C_3N_2H_{12}]$, **IV**^{a}

Moiety	Distance/Å	Moiety	Distance/Å
La(1)–O(1)$^{\#1}$	2.443(3)	La(1)–O(5)	2.578(3)
La(1)–O(2)	2.510(3)	La(1)–O(3)	2.603(3)
La(1)–O(3)$^{\#2}$	2.524(3)	La(1)–O(7)	2.646(3)
La(1)–O(4)	2.529(3)	La(1)–O(8)	2.651(3)
La(1)–O(6)	2.559(3)	La(2)–O(12)$^{\#3}$	2.567(3)
La(2)–O(9)	2.461(3)	La(2)–O(5)$^{\#4}$	2.575(3)
La(2)–O(10)	2.467(3)	La(2)–O(8)	2.589(3)
La(2)–O(6)	2.532(3)	La(2)–O(12)	2.599(3)
La(2)–O(11)	2.552(3)	La(2)–O(7)$^{\#4}$	2.666(3)
S(1)–O(13)	1.446(3)	S(1)–O(5)	1.493(3)
S(1)–O(10)$^{\#3}$	1.470(3)	S(1)–O(8)	1.501(3)
S(2)–O(14)	1.431(3)	S(2)–O(4)	1.485(3)
S(2)–O(9)$^{\#1}$	1.459(3)	S(2)–O(3)	1.497(3)
S(3)–O(15)	1.441(3)	S(3)–O(6)	1.506(3)
S(3)–O(1)	1.463(3)	S(3)–O(7)$^{\#4}$	1.514(3)
S(4)–O(16)	1.446(3)	S(4)–O(2)$^{\#3}$	1.481(3)
S(4)–O(11)	1.480(3)	S(4)–O(12)	1.502(3)

^{a} Symmetry transformations used to generate equivalent atoms: $^{\#1}−x + 1, −y + 1, −z + 1;$ $^{\#2}−x + 1, −y, −z + 1;$ $^{\#3}−x + 2, −y + 1, −z + 1;$ $^{\#4}x, y + 1, z;$ $^{\#5}x, y − 1, z.$

Table 8 Selected bond distances in $[Nd_2(SO_4)_4(H_2O)_4][C_6N_2H_{14}]_2[SO_4][C_2N_2H_8][H_2O]_3$, **V**^{a}

Moiety	Distance/Å	Moiety	Distance/Å
Nd(1)–O(1)	2.429(5)	Nd(1)–O(5)	2.530(4)
Nd(1)–O(2)	2.432(5)	Nd(1)–O(7)	2.535(4)
Nd(1)–O(3)$^{\#1}$	2.485(4)	Nd(1)–O(8)	2.545(4)
Nd(1)–O(4)	2.514(4)	Nd(1)–O(9)$^{\#2}$	2.593(4)
Nd(1)–O(6)	2.529(4)	S(1)–O(4)	1.480(4)
S(1)–O(9)	1.465(4)	S(1)–O(8)	1.489(4)
S(1)–O(7)$^{\#3}$	1.478(4)	S(2)–O(6)	1.480(4)
S(2)–O(10)	1.473(5)	S(2)–O(5)	1.480(5)
S(2)–O(3)	1.473(4)	S(3)–O(12)$^{\#4}$	1.471(6)
S(3)–O(11)	1.443(7)	S(3)–O(12)	1.471(6)
S(3)–O(11)$^{\#4}$	1.444(7)		

^{a} Symmetry transformations used to generate equivalent atoms: $^{\#1}x, −y, z + 0.5;$ $^{\#2}−x + 0.5, y − 0.5, z;$ $^{\#3}−x + 0.5, y + 0.5, z;$ $^{\#4}−x, y, −z + 0.5;$ $^{\#5}x, −y, z − 0.5;$ $^{\#6}−x, −y + 2, −z.$

Results and discussion

Three-dimensional [Ln$_2$(H$_2$O)$_2$(SO$_4$)$_5$][C$_2$N$_2$H$_{10}$]$_2$ (Ln = La, Pr or Nd), I

The asymmetric unit of **I** contains 37 non-hydrogen atoms of which 29 belong to the framework and eight to the organic cation. There are two crystallographically distinct rare-earth metal atoms and five S atoms as can be seen in Fig. 1. The metal atoms are nine-coordinated by the oxygens from four sulfate ions and one water molecule, with each metal atom surrounded by three bidentate sulfate anions and two monodentate sulfate ions. Thus, two of the sulfur atoms in the asymmetric unit, S3 and S5, form four S–O–Ln bonds to two crystallographically distinct Ln atoms, thereby sharing edges with two metal polyhedra. The S1 and S4 atoms form three S–O–Ln bonds to two unique metal atoms, sharing the edge with one metal–oxygen polyhedra and the corner with another, leaving one terminal S–O group. The S2 atom makes two S–O–Ln bonds with two metal atoms, sharing corners with two metal–oxygen polyhedra, and has two terminal S–O groups. Two LnO$_9$ polyhedra are linked by the S(3)O$_4$, S(5)O$_4$ tetrahedra in two-dimensions to form eight-membered rings, the rings connected by S(2)O$_4$ to form layers parallel to the *bc*-plane of the unit cell. Such a connectivity between the eight-membered rings results in the formation of four 16-membered rings around each eight-membered ring (Fig. 2a). The layers are stacked over one another in AAA⋯ fashion, with two adjacent layers separated by a unit cell length along the *a*-axis of the unit cell, thus forming eight and 16-membered channels. The S(1)O$_4$ and S(4)O$_4$ tetrahedra share corners and edges with the metal–oxygen polyhedra respectively from adjacent layers, thereby connecting the layers and forming a three-dimensional framework (Fig. 2b). This connectivity gives rise to a square grid of intersecting eight-membered channels running perpendicular to one another, and intersecting the channels along the *a*-axis of the unit cell.

The protonated amine molecules are located in the cages formed by the intersection of channels in between the layers, with one amine molecule located in the cage formed by the intersection of the three eight-membered channels and three amine molecules in the cages formed by the intersection of the 16-membered channel and two eight-membered channels. The amines form hydrogen bonds with the oxygen atoms of the framework (Table S6†).

The layers formed by the connectivity between the metal–oxygen polyhedra through the sulfate units can be described by a 4.8^2 net obtained by rotating the squares of 4^4 nets with one-fifth vacancies (Fig. 3a) and are comparable to the (001) net of Hg in Pd$_2$Hg$_5$. The entire structure of **I**, along with the
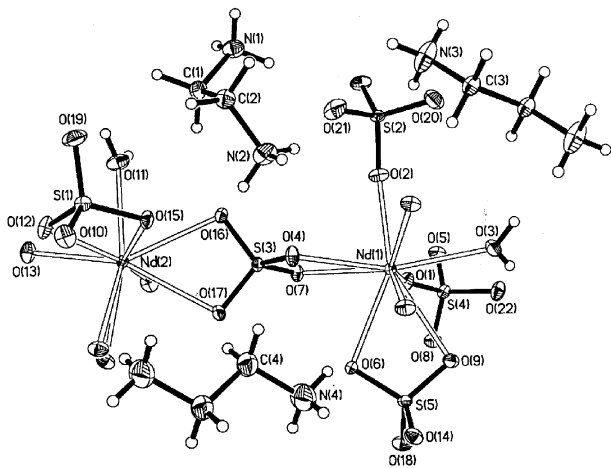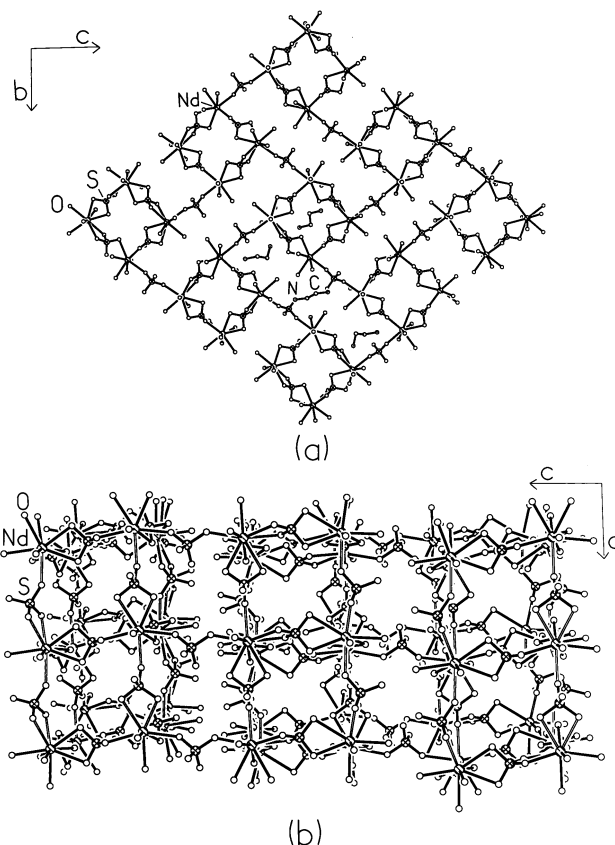

(a)

(b)

Fig. 2 (a) The layer, parallel to the *bc*-plane of the unit cell in **I**, formed by connecting NdO$_9$ polyhedra with SO$_4$ tetrahedra, by sharing edges and vertices, and thereby forming eight-membered and 16-membered rings. Note the arrangement of the 16-membered rings around the eight-membered rings. The protonated amine units are shown in one eight-membered ring and one 16-membered ring. (b) The three-dimensional framework formed by the linking of the layers, stacked one over another, along the *a*-axis of the unit cell by the sulfate groups.

amines, can be compared to the Hg nets in Mn$_2$Hg$_5$ where the Hg atom at the centre of the octagon is replaced by the protonated amine molecules in **I**.[10] The three-dimensional structure itself has the α-polonium type of topology.[10] This can be visualized by comparing the square units formed by the four metal centers linked by the sulfate units as a node. The cuboidal framework formed by eight such interconnected nodes, with each of them being a six-connecting one, can be seen from Fig. 3b. The interpenetration characteristic of α-Po is absent in **I**, probably since the cavities formed within the cubic structures of the network are occupied by the guest moieties.[16]

Three-dimensional [Nd$_2$(SO$_4$)$_4$(H$_2$O)$_2$][C$_4$N$_2$H$_{12}$], II

The asymmetric unit of **II** contains 24 non-hydrogen atoms of which 18 belong to the framework and six to the organic moiety. There are two crystallographically distinct Nd atoms and four S atoms. The Nd atoms have a similar coordination environment, with each having nine-coordination, with eight sulfate oxygens and one water molecule. Thus, each Nd atom is surrounded by three sulfate ions in bidentate and two sulfate ions in monodentate fashion. There are four different sulfate ions in the asymmetric unit. S(2)O$_4$ and S(3)O$_4$ ions have a similar coordination environment, with each forming four S–O–Nd bonds to two crystallographically distinct Nd atoms, thereby sharing edges with two metal–oxygen polyhedra. The S(1)O$_4$ and S(4)O$_4$ ions have a similar coordination environment, with each forming four S–O–Nd bonds. The connectivity between the NdO$_9$ polyhedra by the S(2)O$_4$ and S(3)O$_4$ terahedra results in the formation of eight-membered rings,

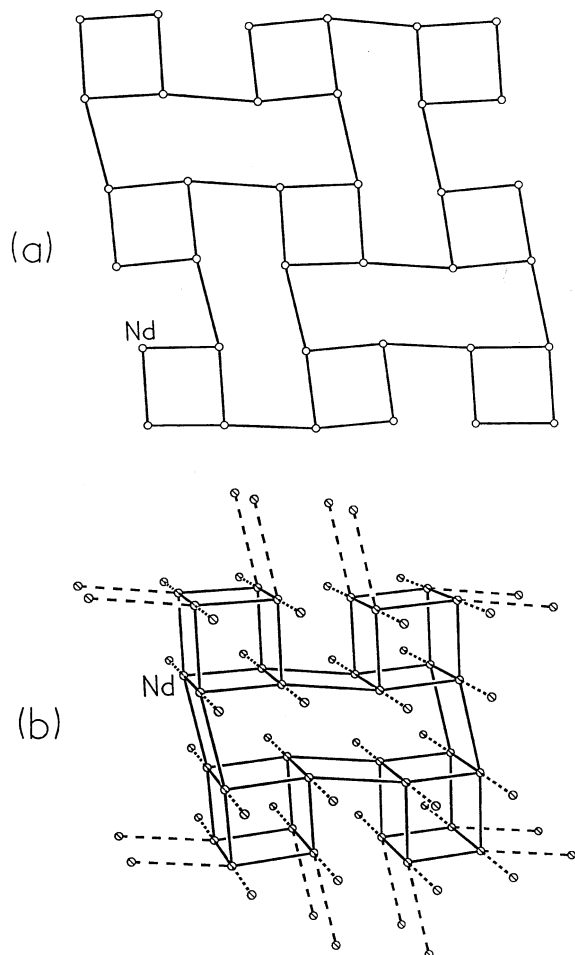**Fig. 1** ORTEP plot of [Nd$_2$(H$_2$O)$_2$(SO$_4$)$_5$][C$_2$N$_2$H$_{10}$]$_2$, **I**. The asymmetric unit is labeled. Thermal ellipsoids are given at 50% probability.

(a)

(b)

Nd

Nd

Fig. 4 The three-dimensional framework in **II**, by the connectivity of the layers, stacked one over another, along the a-axis of the unit cell. Note the eight- and 12-membered channels running down the *a*-axis of the unit cell, with each channel occupied by one piperazinium molecule.

Ln centers results in four-membered rings. Similar four-membered rings are also formed by the connectivity between the $S(1)O_4$ groups and the Ln centers. The four-membered rings get connected by corner sharing, to form the basic building unit in **III** as shown in Fig. 6a. These three-metal center clusters, formed by the corner-sharing of two four-membered rings, join to form a chain running along the *a*-axis

Fig. 3 (a) Representation of the 4.8^2 net sheet parallel to the bc-plane of the unit cell in **I**. (b) Representation of the α-Po related net in the structure of **I**. Note the six connecting squares acting as nodes.

similar to those of **I**. But unlike **I**, the eight-membered rings in **II** get connected by the three-coordinated oxygens of the $S(1)O_4$ and $S(4)O_4$ ions, forming layers parallel to the *bc*-plane of the unit cell. Such a connectivity results in the formation of 12-membered rings around each eight-membered ring (Fig. 4). The presence of three-coordinated oxygens results in the formation of Nd_2O_2 dimers. The layers can also be described as formed by the connectivity of the Nd_2O_2 dimers by the $S(2)O_4$ and $S(3)O_4$ ions. The layers are stacked over one another in AAA··· fashion and get connected by the $S(1)O_4$ and $S(4)O_4$ ions to form the three-dimensional structure. This connectivity between the layers gives rise to eight and 12-membered channels along the *a*-axis of the unit cell, with one protonated piperazine molecule sitting in each of the eight- and 12-membered channels, forming hydrogen bonds with the framework oxygens (Fig. 4).

Layered [Ln₂(SO₄)₄][C₂N₂H₁₀] (Ln = La or Nd), III

The asymmetric unit of **III** contains 12 non-hydrogen atoms of which 10 belong to the framework and two to the organic moiety (Fig. 5a). The Ln atom is nine-coordinated by sulfate oxygens, $S(1)O_4$ forms five S–O–Ln bonds to four different metal atoms leaving one terminal oxygen. Thus, the $S(1)O_4$ tetrahedron shares an edge with one metal–oxygen polyhedron and vertices with three other metal–oxygen polyhedra, and has two three-coordinated oxygens. The $S(2)O_4$ tetrahedron forms 4 S–O–Ln bonds to three different metal atoms and has one three-coordinated oxygen and one terminal oxygen, thereby sharing edges with one and vertices with two metal–oxygen polyhedra. The connectivity between the $S(2)O_4$ ions and the
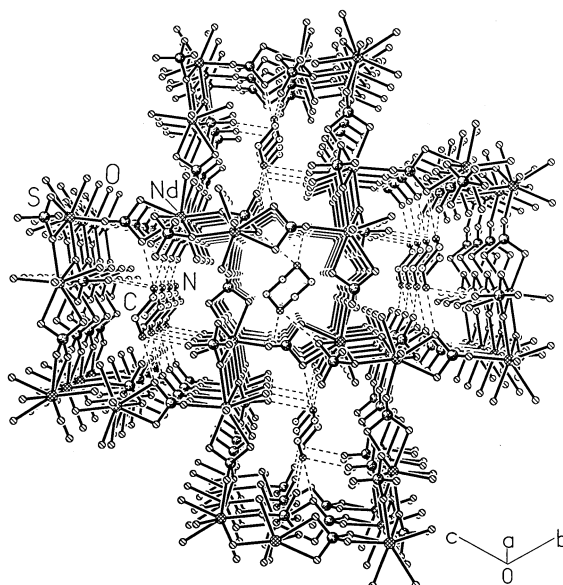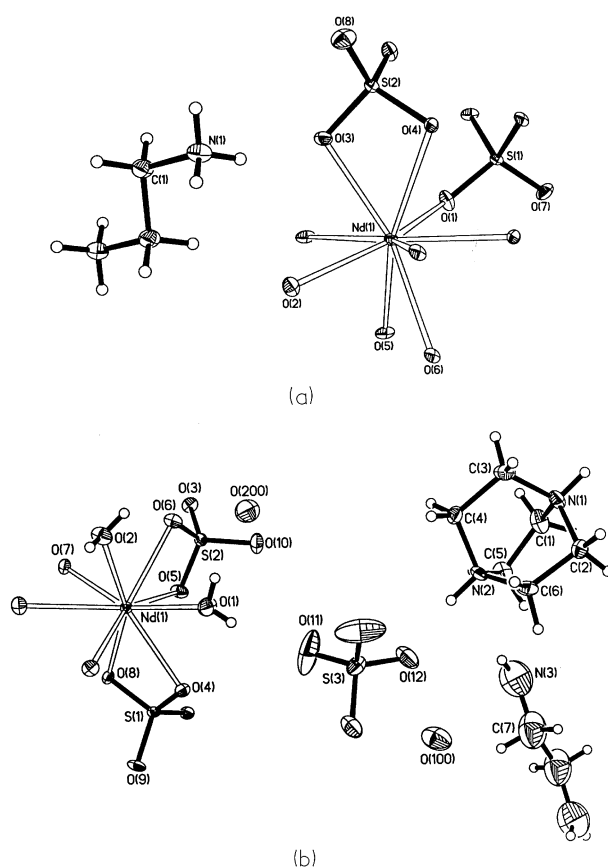

(a)

(b)

Fig. 5 ORTEP plot of (a) $[Nd_2(SO_4)_4][C_2N_2H_{10}]$, **III**, and (b) $[Nd_2(SO_4)_4(H_2O)_4][C_6N_2H_{14}]_2[SO_4][C_2N_2H_8][H_2O]_3$, **V**. The asymmetric unit is labeled. Thermal ellipsoids are given at 50% probability.
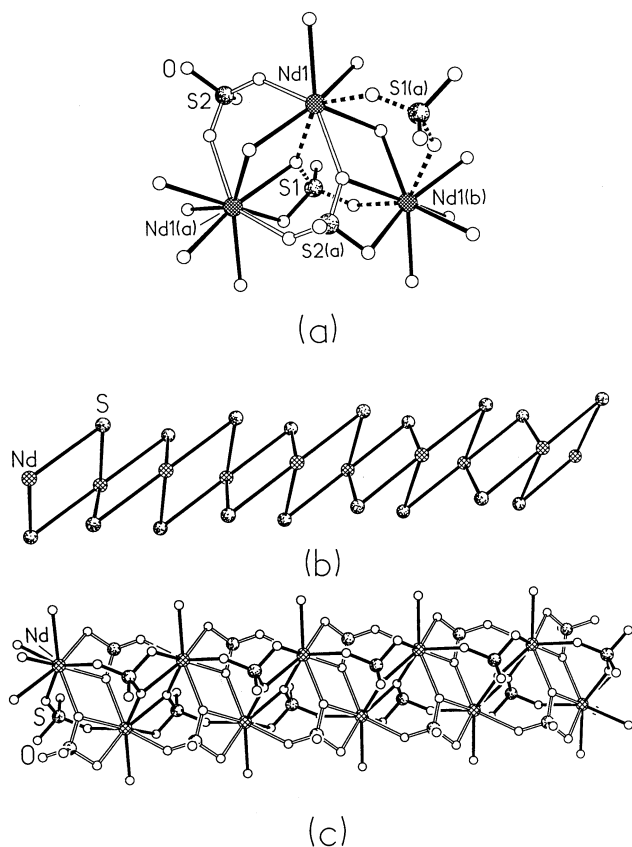
Fig. 6 (a) The three-metal center cluster in **III**, formed by the corner-sharing of two four-membered rings with different sulfate groups, acting as the basic building unit. (b) Chains formed by corner-sharing of four-membered rings. (c) The chain, running parallel to the *a*-axis of the unit cell, formed by joining the basic building units in **III**. Note that each four-membered ring is capped by the three-coordinated sulfate oxygens from the adjacent rings on either side.

Fig. 7 (a) Top view of the layer parallel to the *ab*-plane of the unit cell in **III**, formed by linking of the chains running parallel to the *a*-axis of the unit cell through the three-coordinated oxygen atom of the S(1)O$_4$ group. (b) The infinite two-dimensional Nd–O–Nd linkage in **III**, formed by the bridging of Nd centers by three-coordinated sulfate oxygens. Note the (6, 3) network topology of the NdO$_3$ layer with Nd centers acting as the nodes.

of the unit cell (Fig. 6b). Each four-membered ring is capped by the three-coordinating sulfate oxygens from the adjacent four-membered rings on either side (Fig. 6c). Two such chains, separated by ½ a unit cell length along the *b*-axis of the unit cell, are connected by the second three-coordinated oxygen of the S(1)O$_4$ ion to form layers parallel to the *ab*-plane of the unit cell (Fig. 7a). The connectivity between the chains also results in the formation of four-membered rings in between the chains by the joining of Ln–S(1)–Ln–S(1) through the oxygens, but unlike the four-membered rings in the chains, these rings are uncapped. Thus, the entire layer can be visualized as being formed of two types of four-membered rings – capped four-membered rings forming the chains, which in turn join together to form uncapped four-membered rings in between the chains. The linkages involving the three-coordinated oxygens results in the formation of three-membered rings, and infinite Ln–O–Ln linkages in two-dimensions. Such bridging of the Ln atoms by three-coordinated sulfate oxygens has been observed earlier in lanthanum sulfates,[9,11] but **III** is the first example of an infinite two-dimensional Ln–O–Ln linkage formed by three-coordinated sulfate oxygens. The network formed by the linking of the Ln centers by the three-coordinated oxygens has the composition LnO$_3$ and can be visualized as (6, 3) nets, with each Ln center acting as a node (Fig. 7b).[10]

The anionic inorganic layers in **III** are stacked over one another along the *c*-axis of the unit cell in AAA··· fashion and are separated by a unit cell length along the *c*-axis of the unit cell. The diprotonated ethylenediamine molecules reside in the interlamellar space and form multipoint hydrogen bonds with the framework oxygen atoms from adjacent layers (Fig. 8, also
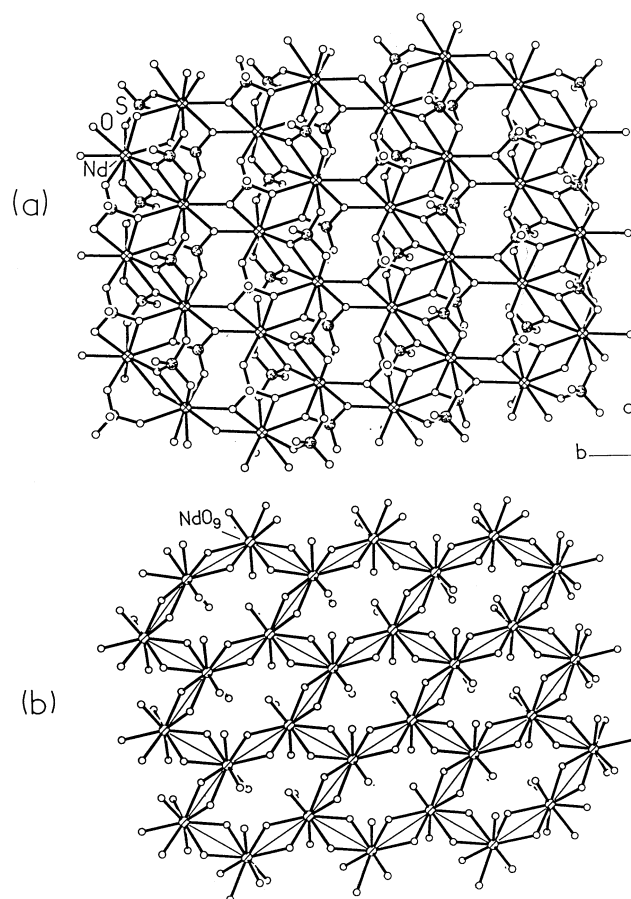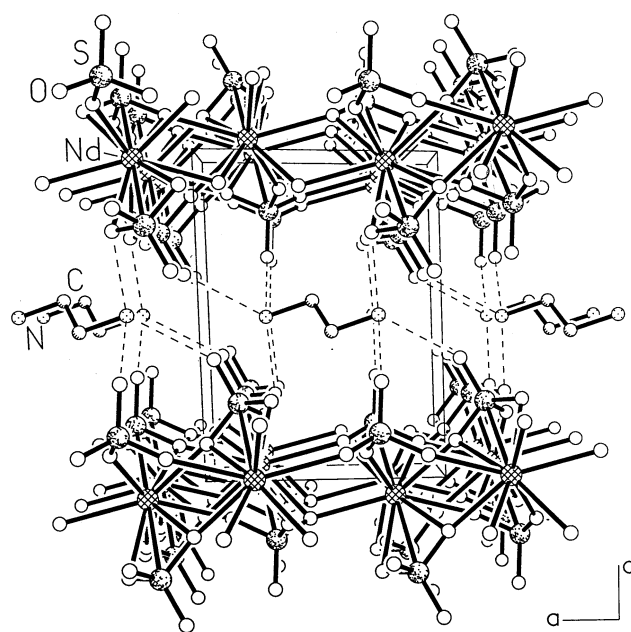

Fig. 8 The stacking of layers in **III**, along the *c*-axis of the unit cell. Note that the entire structure is formed by alternating inorganic and organic layers. Dotted lines represent hydrogen-bond interactions.
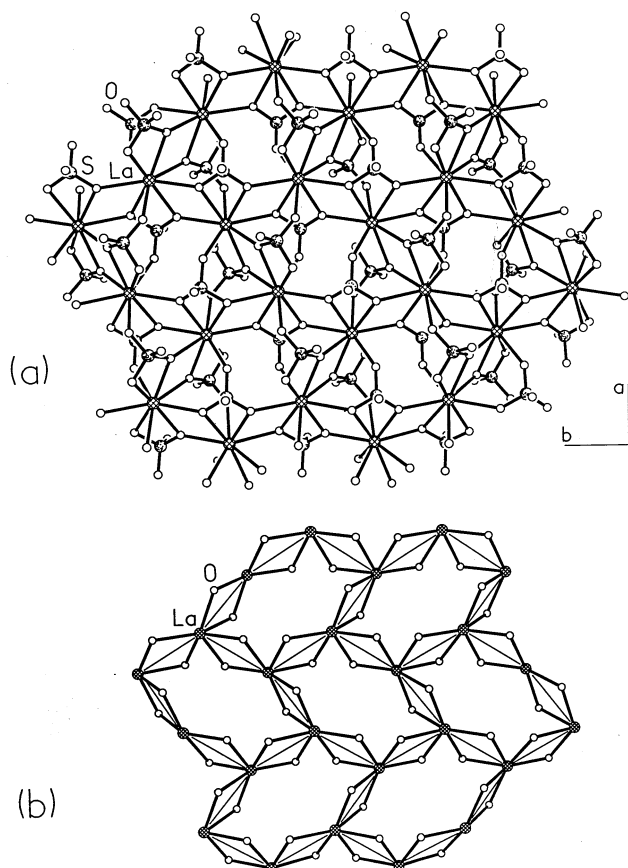
(a)

(b)

Fig. 9 (a) Top view of the layer formed parallel to the *ab*-plane of the unit cell in **IV**, formed by joining of the four-membered ring ladders running parallel to the *b*-axis of the unit cell. Note that alternate four-membered rings of the ladders are capped by the sulfate ions on either side. (b) The infinite two-dimensional La–O–La linkage in **IV**, formed by the bridging of La centers by three-coordinated sulfate oxygens. Note the (6, 3) network topology of the LaO$_3$ layer with La centers acting as nodes, which is different from the (6, 3) NdO$_3$ sheets in **III**.

see table S6†). Thus, the entire three-dimensional structure is made up of alternating anionic inorganic layers and cationic organic layers.

Layered [La$_2$(SO$_4$)$_4$][C$_3$N$_2$H$_{12}$], IV

We have been able to synthesize a layered sulfate of the composition [La$_2$(SO$_4$)$_4$][C$_3$N$_2$H$_{12}$], **IV**, with a structure similar to that of **III**, but differing from **III** in the mode of binding of the sulfate ions, thereby changing the topology of the (6, 3) LaO$_3$ layers. The asymmetric unit of **IV** contains 27 non-hydrogen atoms of which 22 belong to the framework and five to the organic moiety. The La atom is nine-coordinated by the sulfate oxygens. Both S(1)O$_4$ and S(3)O$_4$ form five S–O–La bonds to four different metal atoms, have two three-coordinated oxygens and one terminal oxygen. Thus, the S(1)O$_4$ and S(3)O$_4$ tetrahedra share an edge with one metal–oxygen polyhedron and vertices with three metal–oxygen polyhedra. The S(2)O$_4$ and S(4)O$_4$ tetrahedra have similar coordination environments forming four S–O–La bonds to three different metal atoms, and have one three-coordinated oxygen and one terminal oxygen. The connectivity between the S(1)O$_4$ ions and the La(2) centers results in four-membered rings. The four-membered rings, with La(2) and S(1) as vertices, are connected by sharing of edges to form a ladder structure parallel to the *b*-axis of the unit cell. Alternate four-membered rings of the ladders are capped by S(4)O$_4$ ions on either side which also bridge the La(2) centers through the three-coordinated oxygens. Similar ladders of four-membered rings are formed by the connectivity between La(1) centers and
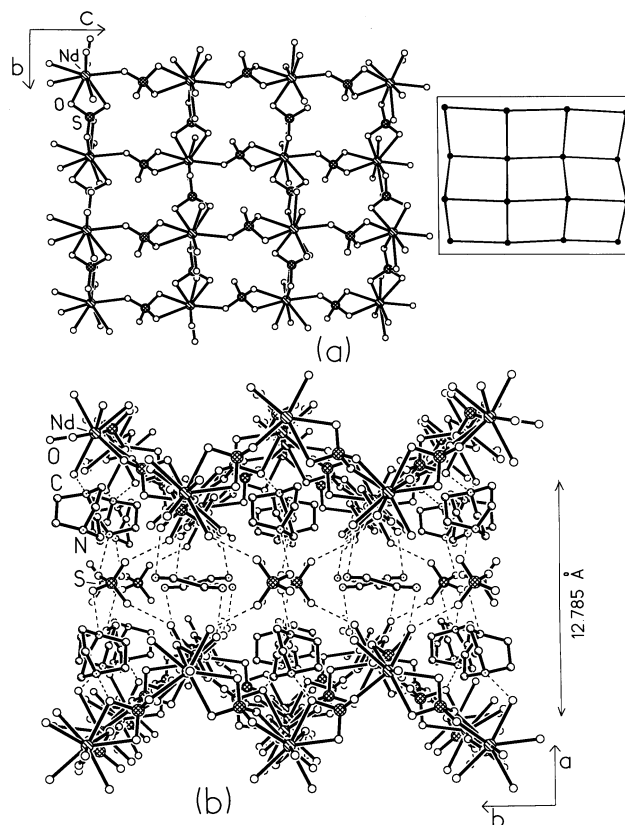

(a)

(b)

Fig. 10 (a) Top view of the layer parallel to the *bc*-plane in **V**, formed by joining the NdO$_9$ polyhedra and SO$_4$ tetrahedra. The inset shows the (4, 4) net sheet formed by the joining of the metal centers. (b) The stacking of the alternate inorganic layers and the layer formed by the ethylenediamine molecules, sulfate ions and the interstitial water molecules, along the *a*-axis of the unit cell. The protonated DABCO molecules reside in the crest and trough regions of the inorganic layer. Dotted lines represent hydrogen-bond interactions. Note the wavelike pattern of the inorganic layers.

the S(3)O$_4$ ions, with the alternate four-membered rings being capped by S(2)O$_4$ ions. The two ladders are stacked alternatively along the *a*-axis of the unit cell and are connected by both the four-membered ring sulfates and capping sulfates to form layers parallel to the *ab*-plane of the unit cell (Fig. 9a). The ring sulfates bind to the metal centers of adjacent ladders through the three-coordinated oxygen atoms, forming infinite La–O–La linkage in two dimensions, giving rise to LaO$_3$ layers of the (6, 3) net topology, with each La center acting as a node (Fig. 9b).[10]

Layered [Ln$_2$(SO$_4$)$_4$(H$_2$O)$_4$][C$_6$N$_2$H$_{14}$]$_2$[SO$_4$][C$_2$N$_2$H$_8$][H$_2$O]$_3$ (Ln = La, Pr or Nd), V

The asymmetric unit of [Ln$_2$(SO$_4$)$_4$(H$_2$O)$_4$][C$_6$N$_2$H$_{14}$]$_2$[SO$_4$]-[C$_2$N$_2$H$_8$][H$_2$O]$_3$, **V**, contains 28 non-hydrogen atoms of which 13 belong to the framework, 10 to two organic moieties, three to the interstitial sulfate ion with S in ½ occupancy and two non-coordinated water molecules (Fig. 5b). The Ln atom is nine-coordinated to three sulfate ions in the bidentate fashion, one sulfate ion in the monodentate fashion and two water molecules. Of the two framework sulfate ions, one binds to two Ln atoms in a bidentate fashion, whereas another binds to one metal atom in a bidentate manner and another in a monodentate fashion leaving a terminal S–O bond (Fig. 5b). The linkage of the LnO$_9$ polyhedra and the SO$_4$ tetrahedra by sharing vertices and edges, gives rise to anionic inorganic layers parallel to the *bc*-plane of the unit cell, containing eight-membered rings (Fig. 10a). The three sulfate tetrahedra sharing edges with the LnO$_9$ polyhedra bind to the Ln atom in a *cis*-fashion rendering the layers corrugated, with the water
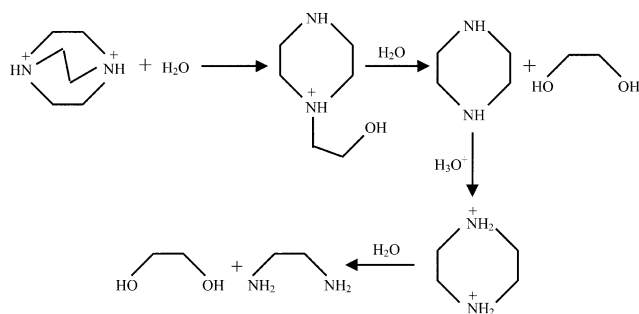
Scheme 1

molecules protruding out of the zig-zag layers. Protonated DABCO molecules reside in the crest and trough regions. The interlayer spacing is 12.78 Å. The sulfate ions and the water molecules along with the ethylenediamine molecules (formed *in situ* by the decomposition of DABCO under the reaction conditions) lie between the inorganic layers (Fig. 10b). Such isolated oxyanions in the interlamellar space have been observed in layered sulfate minerals,[17] in organically templated layered phosphates[18] and in an organically templated layered cadmium sulfate.[6] The amine molecules, the sulfate ions and the interstitial water molecules, form hydrogen bonds among themselves and also with the framework oxygens (Table S6†). The layer formed by the connectivity of the Ln centers by the sulfate units can be visualized as (4, 4) net sheets parallel to the *bc*-plane of the unit cell, with the Ln centers acting as nodes (see inset of Fig. 10a). The entire structure is formed by the stacking of the (4, 4) net sheets along the *a*-axis of the unit cell.[10]

It is somewhat curious that diprotonation of DABCO occurs in **V** and not of ethylenediamine, with more favorable pK_a values. It must be noted, however, that ethylenediamine along with ethylene glycol, would be the product of decomposition of diprotonated DABCO as shown in Scheme 1.

While there may be protonated ethylenediamine molecules in solution, we can have only one diprotonated amine in the interlayer space, because of stoichiometric considerations. It is possible that diprotonated DABCO gives a greater stability to the layer structure, due to a favorable spatial arrangement.

It is interesting to compare the structure of **V** with the structures of β-(NH$_4$)La(SO$_4$)$_2$,[19] (N$_2$H$_5$)Nd(H$_2$O)(SO$_4$)$_2$[20] and La$_2$(H$_2$O)$_2$(C$_2$H$_{10}$N$_2$)$_3$(SO$_4$)$_6$·4H$_2$O.[9] These compounds are built from corrugated anionic layers of rare earth sulfates, with the NH$_4^+$, organic amine and water molecules residing in the interlamellar space and interacting with the layers through hydrogen bonds. In **V**, we have in addition, the sulfate ion in the interlayer space, forming hydrogen bonds with the layers. In all these compounds, the interlamellar spacing depends on the size and orientation of the guest species, the distance increasing from 4.50 Å for ammonium ion to 7.88 Å for hydrazinium ion and to 12.8–13.4 Å for ethylenediammonium ion. The shortest O–O distance between two adjacent layers in **V** is 4.724 Å, which is larger than that in the other three compounds (3.02–3.10 Å), possibly because of the presence of the larger DABCO molecules. It is noteworthy that the layer formed by the ethylenediamine molecules and sulfate ions in **V** is somewhat similar to that in ethylenediammonium sulfate.[21]

Structural parameters

The various bond distances in **I**–**V** are listed in Tables 4–8. The bond lengths for both the LnO$_9$ polyhedra and the SO$_4$ tetrahedra in the above compounds are in agreement with those commonly observed in metal sulfates.[9,11,20,22] The short S–O bond distances corresponded to the terminal S–O groups and the longer S–O bond distances to the S–O bonds involving three-coordinated oxygens.

Conclusions

In conclusion, a variety of open-framework rare earth sulfates templated by amines and possessing either layer or three-dimensional channel structures have been synthesized and characterized. The three-dimensional structure of **I** is comparable to that of α-Po and possesses a grid of intersecting eight-membered channels mutually perpendicular to each other, and also 16-membered channels along one direction. The three-dimensional structure, **II**, with a structure, comparable to that of **I**, contains eight-membered channels joined by Nd$_2$O$_2$ dimers, which results in the formation of four 12-membered channels around each eight-membered channels. We have made three different types of layered structures with (6, 3) or (4, 4) nets. Two of these, **III** and **IV**, containing LnO$_3$ layers with infinite Ln–O–Ln linkages, are formed by the connectivity of the four-membered Ln–S–Ln–S rings either by sharing of corners or edges. A third type of layered structure, **V**, formed by the connectivity of LnO$_9$ polyhedra and SO$_4$ tetrahedra gives rise to (4, 4) nets. In **V** the sulfate ions reside in between the layers in addition to the amine. The present results suggest that it should be possible to design a variety of complex open-framework structures using the sulfate ion as a building block.

References

1 (*a*) D. W. Breck, in *Zeolite Molecular Sieves*, Wiley, New York, 1974; (*b*) W. M. Meier, D. H. Oslen and C. Baerlocher, in *Atlas of Zeolite Structure Types*, Elsevier, London, 1996.

2 (*a*) A. K. Cheetham, G. Ferey and T. Loiseau, *Angew. Chem., Int. Ed.*, 1999, **38**, 3268; (*b*) C. N. R. Rao, S. Natarajan, A. Choudhury, S. Neeraj and A. A. Ayi, *Acc. Chem. Res.*, 2001, **34**, 80.

3 (*a*) B. K. Barthelet, J. Marrot, D. Riou and G. Ferey, *Angew. Chem., Int. Ed.*, 2002, **41**, 281; (*b*) F. Millange, C. Serre and G. Ferey, *Chem. Commun.*, 2002, 822; (*c*) T. M. Reineke, M. Eddaoudi, M. O'Keeffe and O. M. Yaghi, *Angew. Chem., Int. Ed.*, 1999, **38**, 2590 and references therein.

4 (*a*) A. Choudhury, D. Udayakumar and C. N. R. Rao, *Angew. Chem., Int. Ed.*, 2002, **41**, 158; (*b*) W. T. A. Harrison, M. L. F. Philips, J. Stanchfield and T. M. Nenoff, *Angew. Chem., Int. Ed.*, 2000, **39**, 3808; (*c*) D. Udayakumar and C. N. R. Rao, *J. Mater. Chem.*, 2003, **13**, 1635.

5 G. Paul, A. Choudhury, R. Nagarajan and C. N. R. Rao, *Inorg. Chem.*, 2003, **42**, 2004.

6 G. Paul, A. Choudhury and C. N. R. Rao, *J. Chem. Soc., Dalton Trans.*, 2002, 3859.

7 (*a*) G. Paul, A. Choudhury, E. V. Sampathkumaran and C. N. R. Rao, *Angew. Chem., Int. Ed.*, 2002, **41**, 4297; (*b*) G. Paul, A. Choudhury and C. N. R. Rao, *Chem. Commun.*, 2002, 1904.

8 P. M. Thomas, A. J. Norquist, M. B. Doran and D. O'Hare, *J. Mater. Chem.*, 2003, **13**, 88.

9 T. Bataille and D. Louër, *J. Mater. Chem.*, 2002, **12**, 3487.

10 (*a*) A. F. Wells, in *Three-Dimensional Nets and Polyhedra*, Wiley Interscience, New York, 1977; (*b*) M. O'Keeffe and B. G. Hyde, *Philos. Trans. R. Soc. London*, 1980, **A295**, 553; (*c*) S. R. Batten and R. Robson, *Angew. Chem., Int. Ed.*, 1998, **11**, 1460.

11 Y. Xing, Z. Shi, G. Li and W. Pang, *Dalton. Trans.*, 2003, 940.

12 (*a*) J. Selbin, L. H. Holmes and S. P. McGlynn, *J. Inorg. Nucl. Chem.*, 1963, **25**, 1359; (*b*) K. Nakamoto, in *Infrared and Raman Spectra of Inorganic and Coordination Compounds*, Wiley Interscience, New York, 1978.

13 (*a*) G. M. Sheldrick, SHELXS-86 Program for Crystal Structure Determination, University of Gottingen, Gottingen, Germany, 1986; (*b*) G. M. Sheldrick, *Acta Crystallogr., Sect. A*, 1990, **46**, 467.

14 G. M. Sheldrick, SADABS: Siemens Area Detector Absorption Correction program, University of Gottingen, Gottingen, Germany, 1994.

15 G. M. Sheldrick, SHELXS-93 Program for Crystal Structure Solution and Refinement, University of Gottingen, Gottingen, Germany, 1993.

16 Y. –B. Dong, M. D. Smith and H-C. Z. Loye, *Angew. Chem., Int. Ed.*, 2000, **39**, 4271.

17 F. C. Hawthrone, S. V. Krivovichev and P. C. Burns, *Rev. Miner. Geochem.*, 2000, **40**, 1.

18 (*a*) N. Simon, T. Loiseau and G. Ferey, *J. Mater. Chem.*, 1999, **9**,

585; (*b*) A. Choudhury, *Proc. Indian Acad. Sci. (Chem. Sci.)*, 2002, **114**, 93.

19 P. Benard-Rocherulle, H. Tronel and D. Louer, *Powder Diffr.*, 2002, **17**, 290.

20 S. Govindarajan, K. C. Patil, H. Manohar and P. –E. Werner, *J. Chem. Soc., Dalton Trans.*, 1986, 119.

21 K. Jayaraman, A. Choudhury and C. N. R. Rao, *Solid State Sci.*, 2002, **4**, 413.

22 (*a*) D. Louër, T. Rius and P. Benard-Rocherulle, *Powder Diffr.*, 2002, **17**, 210; (*b*) D. Koppikar, P. V. Sivapullaiah, L. Ramakrishnan and S. Soundarajan, *Struct. Bonding (Berlin)*, 1978, **34**, 1195.